Noname manuscript No.
(will be inserted by the editor)

Fuzzy Tuned PID controller for Envisioned Agricultural Manipulator

Satyam Paul · Ajay Arunachalam · Davood Khodadad · Henrik Andreasson · Olena Rubanenko

Received: date / Accepted: date

Abstract The implementation of image-based phenotyping systems has become an important aspect of crop and plant science research which shown tremendous growth over the years. Accurate determination of features using images requires stable imaging and very precise processing. By installing a camera on a mechanical arm with a motor, maintaining accuracy and stability is very challenging and non-trivial. As per the state-of-the-art, the issue of external camera shake due to vibration is a great concern in grabbing accurate images, which may be induced by the driving motor of the manipulator. So there is a requirement of a stable active controller for sufficient vibration attenuation of the manipulator. However, there are very few reports in agricultural practice which use control algorithms. Although many control strategies have been utilized to control the vibration in manipulator associated to various ap-

Satyam Paul
Department of Engineering Design and Mathematics,
University of the West of England, Bristol, United Kingdom
E-mail: satyam.paul@uwe.ac.uk

Ajay Arunachalam
Centre for Applied Autonomous Sensor Systems (AASS),
Örebro University, Sweden
E-mail: ajay.arunachalam@oru.se, ajay.arunachalam08@gmail.com

Davood Khodadad
Department of Applied Physics and Electronics,
Umeå University, Umeå, Sweden
E-mail: davood.khodadad@umu.se

Henrik Andreasson
School of Science and Technology,
Örebro University, Örebro, Sweden
E-mail: henrik.andreasson@oru.se

Olena Rubanenko
Regional Innovational Center for Electrical Engineering,Faculty of Electrical Engineering
University of West Bohemia, Pilsen,Czech Republic
E-mail: rubanenk@rice.zcu.cz

plications, no control strategy with validated stability have been provided to control the vibration in such envisioned agricultural manipulator with simple low-cost hardware devices with the compensation of nonlinearities. So, in this work, the combination of PID control with Type-2 fuzzy logic (T2-F-PID) is implemented for vibration control. The validation of the controller stability using Lyapunov analysis is established. Torsional Actuator (TA) is applied for mitigating torsional vibration, which is a new contribution in the area of agricultural manipulator. Also, to prove the effectiveness of the controller, the vibration attenuation results with T2-F-PID is compared with conventional PD/PID controllers and type-1 fuzzy PID (T1-F-PID) controller.

Keywords PID controller · Fuzzy Logic · Precision Agriculture · Vibration Control · Stability Analysis · Robotic Arm · Digital Agriculture · Manipulator Arm · Camera · Mechanical Arm · Raspberry Pi · type-2 fuzzy · CNC Farming

1 Introduction

1.1 Precision Agriculture System & Role of Phenotyping

Plants life plays a crucial role serving the conduit of energy into the biosphere, provide food, and shape our environment. With the growth of new technologies plant science has seen tremendous transformation. [1] identify the role of technologies to address the challenges of new biology. But, with climate change being a major concern, the outdoor farming is more threatened then before, and further fertile land is a limited resource globally now. Approximately, a quarter of worlds CO2 emission comes from food production, and the global climate impact of agriculture is increasing day-by-day. The irony is that agriculture itself is the main contributor to climate change, which in-turn is severely affected by it. Scaling the food production to meet the future human demands, without compromising the quality, while also targeting sustainability is non-trivial. One can just imagine the magnitude, like over the next 40 years, mankind must produce as much food as man has done in total over past several 1000 years. This brings the need for significant increase of the yield production. United Nations estimates that the world population will rise from around 7.8 billion today to around 10 billion by 2050. The world will need lot more food, and the farmer community will face serious treat and challenge to keep up with demand with mounting pressure majorly due to climate change. So, this brings to the need for food cultivation change, i.e., Cyber Agriculture/Vertical Farming/Urban Farming, while aiming sustainability over time. Certainly, the trend is towards indoor cultivation [2][3][4]. But, then just remote indoor farming is not the ultimate solution. There is always a need for organized indoor cultivation for maximizing the harvest on a smaller compatible surface with optimized usage of resources, thereby preparing us today for the global needs of better tomorrow. We discuss one such prototype (LOMAS++) (See Fig. 1.) aimed for autonomous organized cultivation [5].

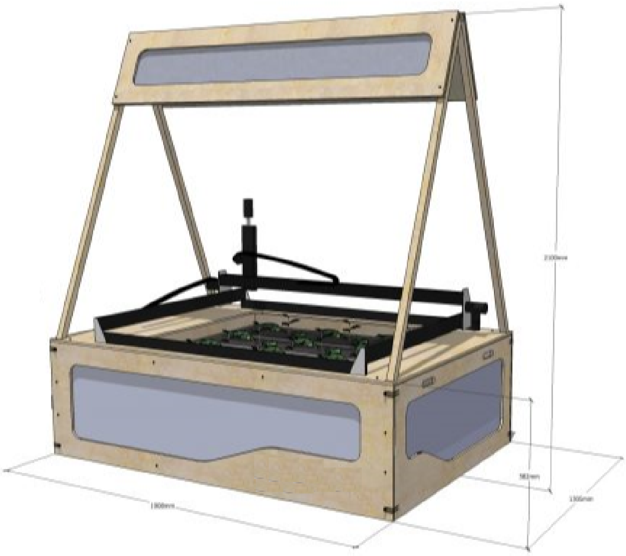

Fig. 1 Autonomous CNC Cultivation Test-bed, Copyright [6]

The project is carried out in collaboration between Alfred Nobel Science Park, and AASS, Örebro University, Örebro, Sweden. LOMAS++ is an autonomous multifunctional farming cultivation bed, aimed for high quality indoor growth and monitoring of plants, with an aim to optimize the cultivation, while producing high quality yields. It opens a new research dimension at Örebro University. Further, it also provides a unique opportunity for the students to use the prototype for academic purposes.

In general, Plant Phenotyping refers to the use of digital and non-invasive technologies to interpret the physical properties observed in plants. Examples include appearance, development, and reciprocal behavior, etc. Practise and understanding of agriculture has seen wide use of vision-based technologies. Plant Phenotyping methods based on image processing have received much attention in recent years [7] [8]. Such, systems have been developed as a result of technology advancement, and the advent of various types of low-cost devices. The advantage of such approaches have key important aspects such as being non-destructive in nature, gaining high-throughput data continuously, etc. From traditional to advanced traits, are obtained from images [9] which provides crucial information revealing the plant health and stress status.

Agricultural robots are becoming a common part of modern farming methods. Nowadays, many operations of sorting, sorting and packing, spraying pests and controlling pests and weeds, detecting harvest time and existing diseases are done automatically with the intervention of agricultural robots [10]. Further, these robots have been used in different magnitudes from small scale to heavy duty applications [11]. The agricultural robots market is roughly expected to reach around 12 billion USD within next 5 years. Articulated robotic arm have been widely used in most of these applications. The robot arm typically has different connections that can move at greater angles and move up or down. This is while the human arm can move (upwards) only in one direction by taking the reference of the straight arm. As an example, we can mention the articulated arm in [12].

The vulnerability of cameras mounted on such articulated robot arms is greater. Also, as a result of camera movement, camera shake and poor focus during exposure, the image loses its quality dramatically. Therefore, camera shake resulting from the running of the motors cause serious concerns in such image acquisitions. [13] studies the blur originating from the camera shake using the statistics of acquired images of the shaken camera in order to predict perceptual blur.

Industrial manipulations have been widely used in the past as known as the robotic arm. Controlling and stabilizing such manipulations is still a topic of current researches. The robustness of PID controllers against noise and other vibration-related parameters facilitates and justifies its application for practical control issues [14] studies the motion of a 6-DoF robot, regardless of its cause such as force and torque. Control algorithms are widely used in many industries. One of them is structural vibration control. [15] shows that a uniform exponential stability can be achieved by using a mechanically implemented damping device. But, then the active control becomes a non-trivial task, when it is non-linear in nature [16]. Victor et al. [17] proposed a scheme a scheme that benefit of smooth function (instead of using the sign function) uses sliding-mode controller in order to alleviate the uncertainty and also disturbances for flexible link robotic manipulators. Neural networks also have been applied to various control problems like Khalil et al.[18] proposed a neuro-controller to stabilize inverted arm, where the validation of their method was done using Simulink simulations. In the work by He et al.[19], a neural network (NN) controller is developed to minimize the vibration forces on the flexible robotic manipulator system associated to input deadzone. A distinguishing model on the basis of nonlinear golden section adaptive control technique is developed for vibration minimization of a flexible Cartesian smart material manipulator which is initiated with the help of ballscrew mechanism combined with AC servomotor [20]. A combined fuzzy+PI technique for active vibration attenuation of a flexible manipulator combined with PZT patches was presented by Wei et al. [21]. A dynamic modeling and an innovative vibration control strategy for a Nonlinear Three-Dimensional Flexible Manipulator was presented by Liu et al. [22]. Yavuz et al. [23] presented the vibration control of a single-link flexible composite manipulator using motion profiles. The trapezoidal and triangular velocity profiles are considered for the motion commands. Matsumori et al.[24] proposed an operato based nonlinear vibration attenuation technology utilizing a flexible arm in combination with shape memory alloy. The effectivity of the proposed methodology is validated by simulations and experiments.An improvised quantum-inspired differential evolution termed as MSIQDE algorithm on the basis of Mexh wavelet function, standard normal distribution, adaptive quantum state update as well as quantum non-gate mutation is suggested by Deng et al. [25] for the avoidance of premature convergence and to upgrade global search capability. The abilities of the MSIQDE-DBN technique is verified by using the vibration data of rolling bearings from the Case Western Reserve University.

The concept of fuzzy logic has become extremely popular due to its nonlinear mapping capability and can be used in various systems while maintaining robustness and simplicity. Therefore, due to the nature of robust and effective nonlinear mapping, fuzzy logic has found wide and increasing applications. Tong et al.[26] provided an investigation on the adaptive fuzzy output feedback backstepping control design problem associated with uncertain strict-feedback nonlinear systems in the presence of unknown virtual as well as actual control gain functions with non measurable states. A novel adaptive fuzzy output feedback control methodology on the basis of backstepping design is illustrated by Tong et al. [27] for a class of SISO strict feedback nonlinear systems with unmeasured states, nonlinear uncertainties, unmodeled dynamics, as well as dynamical disturbances. The technique of fuzzy logic is implemented for the approximation of the nonlinear uncertainties. The state estimation is carried using adaptive fuzzy state observer. Liu et al. [28] proposed a fuzzy proportional-integral-differential (PID) control technique in order to initiate the space manipulator track the required trajectories in different gravity environments. The combination of fuzzy methodology with PID control is implemented to develop the novel methodology. PID controller parameters are tuned on line based on fuzzy controller. An innovative control strategy of a two-wheeled machine with two-directions handling mechanism in combination with PID and PD-FLC algorithms was presented by Goher et al. [29]. Two control methodology was developed for stabilizing the systems highly nonlinear model. The use of an additional DOF embedded in type-2 fuzzy logic as a footprint of uncertainty makes it perform better than a type-1 fuzzy logic system [30][31]. The main concept and the technical content of fuzzy logic type-2 is shown in [32]. Due to the fact that fuzzy logic type-2 has a better performance capacity than fuzzy logic type-1, it is then used as one of the efficient methods of compensating the uncertainty [33]. In the work of Paul et al. [34], it was demonstrated that in the control of vibration of the structure, the type-2 fuzzy PD/PID controller performs better than the classical fuzzy PD/PID controller. Combining type-1 and type-2 fuzzy logic systems, an innovative method has been proposed and the performance of the proposed method is also demonstrated in pitch angle controlled wind energy systems. The results show that the type-2 fuzzy logic system offers better performance in comparison to type-1 fuzzy logic systems [35]. There is another comparison between the performance of the two types which is implemented in laser tracking system by Bai et al. [36]. Sun et al. [37] used Type-2 fuzzy model to control the overall stability of multilateral tele-operation system, where the uncertainties are compensated with fuzzy-model-based state observer.

Fig. 2 Developed Low-cost MultiSpectral Camera, Copyright [6]

1.2 Motivation of this work

As a part of the ongoing research project, an Low-cost Multispectral camera setup was designed as shown in Fig. 3, which is mounted over an mechanical manipulator arm as seen in Fig. 4. The manipulator arm under consideration has 2-DoF as highlighted in Fig. 5. Currently, the present setup (as seen in Fig. 4) is manual, where the camera Field Of View (FOV) is adjusted by the human operator according to the crop/plant species being inspected to get best view of the entire testbed. With an vision to automate the present setup, where the arm will be motor driven, that aim to capture images, while either in continuous motion or discrete motion to get a closer view of the Region Of Interest (ROI) during the operation demands stable vibration control.

While, on the contrary using any industrial state-of-the-art robot arm like Panda 7-DoF from Franka Emika [38] that is widely used by the robotics community will work perfectly for achieving an position-based visual servoing as the feedback information extracted from the vision sensor is used to control the motion of the robot. But, then the trade-off becomes the cost of acquiring one such commercial setup (Avg. 10,500 USD). If the external camera block is shaken originating from movements, it will lead to poor image quality. Such vulnerabilities can generally be controlled offline or online [39]. In the past, researchers have focused on the first method, which required the use of sophisticated algorithms to perform various steps to create, enhance images, remove noise, and calibrate the camera offline. On the other hand, the second method for instant applications was and is more suitable. The work done in the past for online processing focused more on the use of sophisticated online algorithms. They were computationally overloaded. Therefore, given that our goal is to move towards mechanization of the current settings, we decided to study this issue in terms of hardware where control algorithms can be used to eliminate vibrations caused by the motor. For real-time applications or scenarios, an effective controller should be simplistic, robust, and resilient. Proportional

Fig. 3 Mounted Setup, Copyright [6]

Derivative (PD) control as well as Proportional-Integral-Derivative (PID) control is implemented widely in different domains as it is the best control strategy, because it demonstrates its effectiveness without knowledge of the model.

While several control techniques were used to control the vibration in the manipulator in different applications, no validated stability control technique was given to control the vibration in such envisaged agricultural manipulator with simple low-cost hardware system with nonlinearity compensation. So this the main motivation of this research. Based on the motivation, the main contribution of this work are: 1) The combination of PID control with Type-2 fuzzy logic (T2-F-PID) is an innovative way, and first of its kind for this application for vibration control. 2) The validation of the controller stability using Lyapunov analysis for the agricultural application. 3) The implementation of Torsional Actuator (TA) for mitigating torsional vibration is a new contribution in the area of agricultural manipulator. Also, to prove the effectiveness of the controller, the vibration attenuation results with T2-F-PID is compared with conventional PD/PID controllers and type-1 fuzzy PID (T1-F-PID) controller. The entire vibration control scheme is represented by Fig. 5.

The paper is organized as follows. Section 2 describes the way the manipulator arm is controlled using the PID controller. The same is justified with mathematical analysis in Section 3. In Section 4 the proposed model is validated. Related Works are enlisted in Section 5. And, finally, we conclude the paper in Section 6.

Fig. 4 Manipulator Arm with 2-DoF being manually operated

2 Type-2 Fuzzy Modeling of Manipulator

The polar moment of inertia of a DC motor as shown in Fig. 6 is given by:

$$P_t = m_m r_m^2 \tag{1}$$

where, m_m signifies motor mass and r_m signifies motor radius. Generated motor torque is represented as:

$$\tau = P_t \ddot{\theta} - F_f \tag{2}$$

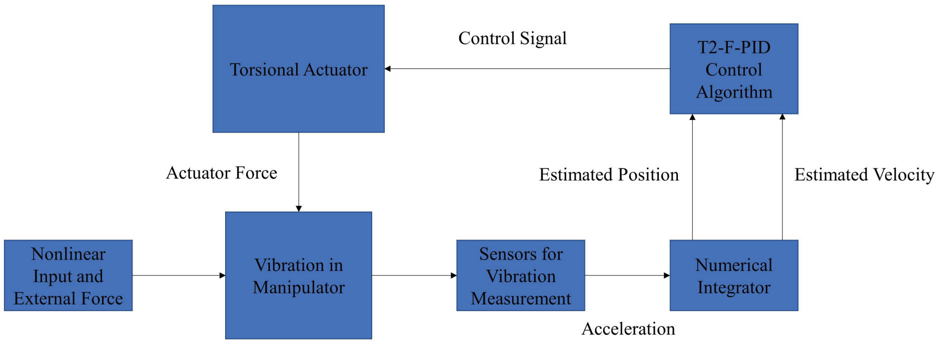

Fig. 5 Vibration Control Scheme of the Manipulator

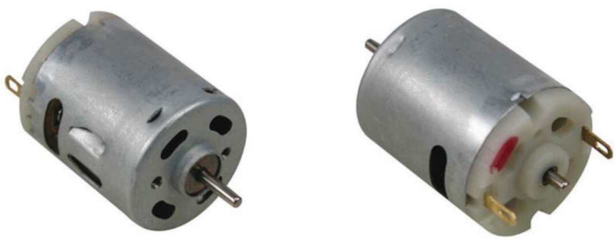

Fig. 6 Schematic of DC motor

where the motor angular acceleration is represented by $\ddot{\theta}$ and F_f is the frictional torque. The mathematical model of the manipulator having rotational motion due to the motor is:

$$P_t\ddot{\theta} + D_\theta\dot{\theta} + S\theta = f_e \tag{3}$$

where θ is the angular position, P_t is the polar moment of inertia, D is the damping force, S is the stiffness force vector, and $\mathbf{f}_e$ is the external force on the manipulator. The manipulator with motor arrangements is shown in Fig. 7.

Now let u_θ be the control force require to attenuate the torsional vibration. For minimization of vibration along theta direction, a torsion actuator (TA),

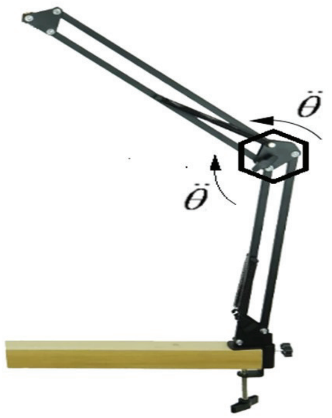

Fig. 7 Manipulator with motor arrangement

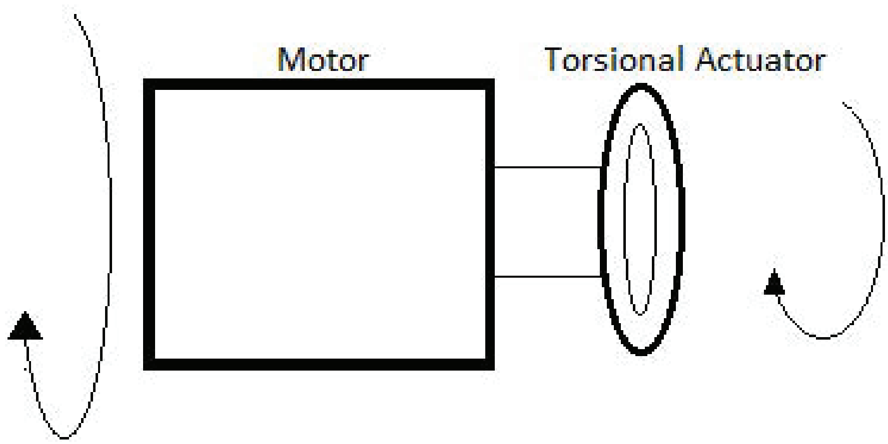

Fig. 8 The placement of TA

is positioned at the physical center of the motor box arrangement, see Fig 8. The TA is a rotating disc like structure combined with a DC motor. The modeling equation of the manipulator (3) with the control force u_θ is:

$$P_t\ddot{\theta} + D_\theta\dot{\theta} + S\theta = f_e + u_\theta - F_{ta} \quad (4)$$

where F_{ta} is the damping and friction force vector associated with the torsional actuator. The torque T_τ generated by the torsional actuator is [40]:

$$T_\tau - F_{ta} = P_{ta}(\ddot{\theta}_{ta} + \ddot{\theta})$$

where P_{ta} is the polar moment of inertia of the TA, $\ddot{\theta}_{ta}$ is the angular acceleration of the TA . The friction in the torsional actuator is:

$$F_{ta} = C\dot{\theta} + (F_c + F_{cs} \sec h(H\dot{\theta})) \tanh(B\dot{\theta})$$

where C and F_c represents torsional viscous friction coefficient and Coulomb friction torque respectively, F_{cs} is the Striebeck effect component. Also, H and B are the dependent variables associated to F_{cs} and F_c respectively. The closed loop system (4) becomes

$$P_t\ddot{\theta} + D_\theta\dot{\theta} + S\theta + C\dot{\theta} + (F_c + F_{cs} \sec h(H\dot{\theta})) \tanh(B\dot{\theta}) - f_e = u_\theta \quad (5)$$

Now in eqn. (5), u_θ is the control force to be fed to the torsional actuator for the vibration control which is equivalent to the torque force $P_{ta}(\ddot{\theta}_{ta} + \ddot{\theta})$.

The term $C\dot{\theta} + (F_c + F_{cs} \sec h(H\dot{\theta})) \tanh(B\dot{\theta}) - f_e$ involves nonlinearity and has to be dealt in an effective manner. Now the nonlinear term can be expressed as follows:

$$f_\theta = C\dot{\theta} + (F_c + F_{cs} \sec h(H\dot{\theta})) \tanh(B\dot{\theta}) - f_e \quad (6)$$

So the eqn. (5) is:

$$m_m r_m^2 \ddot{\theta} + D_\theta\dot{\theta} + S\theta + f_\theta = u_\theta \quad (7)$$

For handling the nonlinearities, Type-2 fuzzy logic system is implemented.The type-2 fuzzy sets can model uncertainties with less fuzzy rules and with greater ease.

The type-2 fuzzy sets has advantages over type-1 fuzzy sets as type-2 fuzzy involves less fuzzy rules in dealing uncertainities effectively. Here $\tilde{T}$ denotes Type-2 Fuzzy set, where the characterization occurs by the Type-2 membership function $M_{\tilde{A}}(\theta, u_\theta)$ [41,42]:

$$\tilde{T} = \{(\theta, u_\theta), M_{\tilde{A}}(\theta, u_\theta) \mid \forall\ \theta \epsilon \Theta, \forall\ u_\theta \epsilon P_\theta \subseteq [0\ 1]\} \quad (8)$$

also, $0 M_{\tilde{A}}(\theta, u_\theta) 1$. where P_θ is considered as the primary membership of θ. One of the crucial part is the Footprint of uncertainty (*FoU)* termed to be the union of associated primary memberships

$$FoU(\tilde{T}) = U_{\theta\epsilon\Theta} P_\theta \quad (9)$$

The *IF-THEN* rules implemented for type-2 fuzzy logic bears the same structure as Type-1 fuzzy logic counterpart. This technique demands that the antecedents as well as the consequents are described by implementing interval Type-2 Fuzzy sets. Hence, l^{th} rule is, [43]: $\mathrm{R}^l : IF(\theta is \tilde{F}_1^l) and (\dot{\theta} is \tilde{F}_2^l)$

$THEN(f_\theta is \tilde{H}_1^l)$ where $\tilde{F}_1^l, \tilde{F}_2^l$, and $\tilde{H}_1^l$ represents Fuzzy sets. For the implementation of the centroid methodology when combined with the center-of-sets type reduction technique, the fuzzy sets associated with the type-2 technique can be converted to an interval type-1 Fuzzy sets $[y_{lk}^z \; y_{rk}^z]$ by taking into consideration each rule of z. The deduced interval Type-1 Fuzzy set is represented as:

$$y_{lk} = \frac{\sum_{z=1}^{L} f_l^z y_{lk}^z}{\sum_{z=1}^{L} f_l^z}, y_{rk} = \frac{\sum_{z=1}^{L} f_r^z y_{rk}^z}{\sum_{z=1}^{L} f_r^z} \tag{10}$$

where $f_l^z \; f_r^z$ denotes the firing strengths linked to y_{lk}^z and y_{rk}^z of rule i. In the first instance, the extraction of type-reduced set is achieved by utilizing left most and right most points y_{lk} and y_{rk}. Once the above step is accomplished,the defuzzification occurs by utilizing interval set type average formula in order to extract the crisp output. The output associated with the fuzzy technique $\hat{f}_\theta$ can be expressed by using singleton fuzzifier as: [44]:

$$\begin{array}{c} \hat{f}_\theta = \frac{y_{right}+y_{left}}{2} \\ \hat{f}_\theta = \frac{1}{2}\left[\phi_r^T(z_\theta)w_r(z_\theta) + \phi_l^T(z_\theta)w_l(z_\theta)\right] \end{array} \tag{11}$$

where $z = \left[\theta \; \dot{\theta}\right]^T$.

3 Type-2 Fuzzy Modeling of Manipulator

PID controllers use the feedback technique approach, which has three interconnected actions:

P : to increase the response velocity;

D : for the purpose of damping;

I: to achieve a required steady-state response.

A PID control is illustrated as

$$\mathbf{u}_{pid} = -K_p\mathbf{e} - K_i\int_0^t \mathbf{e}d\tau - K_d\dot{\mathbf{e}} \tag{12}$$

where the gains of the PID controller are represented by K_p, K_i and K_d and they are positive definite in nature. e is the error stated as $e = \theta - \theta^d, \dot{e} = \dot{\theta} - \dot{\theta}^d$. For the reference, $\theta^d = \dot{\theta}^d = 0$. Therefore,

$$e = \theta, \dot{e} = \dot{\theta}$$

When type-2 fuzzy technique is combined with the PID controller then the outcome is:

$$u_\theta = -K_p\theta - K_i\int_0^t \theta d\tau - K_d\dot{\theta} - \frac{1}{2}\phi_r^T(z_\theta)w_r(z_\theta) - \frac{1}{2}\phi_l^T(z_\theta)w_l(z_\theta) \tag{13}$$

The closed loop equation can be extracted from (7) and (13):

$$m_m r_m^2 \ddot{\theta} + D_\theta \dot{\theta} + S\theta + f_\theta = -K_p\theta - K_i \int_0^t \theta d\tau - K_d\dot{\theta} - \frac{1}{2}\phi_r^T(z_\theta)w_r(z_\theta) - \frac{1}{2}\phi_l^T(z_\theta)w_l(z_\theta) \tag{14}$$

Let, $K_i \int_0^t \theta d\tau = I_\theta$, then

$$\begin{aligned} \dot{I}_\theta &= K_i\theta \\ \frac{d}{dt}(\theta) &= -\left(m_m r_m^2\right)^{-1}[D_\theta\dot{\theta} + S\theta + f_\theta + K_p\theta + K_d\theta + I_\theta \\ &\quad + \tfrac{1}{2}\phi_r^T(z_\theta)w_r(z_\theta) + \tfrac{1}{2}\phi_l^T(z_\theta)w_l(z_\theta)] \end{aligned} \tag{15}$$

where I_θ is the auxiliary variable. In matrix form, (15) is

$$\frac{d}{dt}\begin{bmatrix} I_\theta \\ \theta \\ \dot{\theta} \end{bmatrix} = \begin{bmatrix} K_{ix}\theta \\ \dot{\theta} \\ -\left(m_m r_m^2\right)^{-1}[D_\theta\dot{\theta} + S\theta + f_\theta + u_\theta] \end{bmatrix} \tag{16}$$

From (14) it is justified that the origin is not at the equilibrium and is in the format $\left[\theta\dot{\theta}I_\theta\right] = \left[\theta\dot{\theta}I_\theta^*\right]$.Since at equilibrium point $\theta = 0, \dot{\theta} = 0$, then the equilibrium is

$$[0, 0, \lambda_\theta(0, 0)]$$

where $I_\theta^* = I_\theta - \lambda_\theta(0, 0)$. Using Stone-Weierstrass theorem (Bernhard and Mulvey, 1997), f_θ can be estimated as:

$$f_\theta = \frac{1}{2}\phi_r^T(z_\theta)w_r^*(z_\theta) + \frac{1}{2}\phi_l^T(z_\theta)w_l^*(z_\theta) + \lambda_\theta \tag{17}$$

where the model error is represented by λ_θ and

$$\begin{aligned} \tilde{w}_r(z_\theta) &= -[w_r(z_\theta) + w_r^*(z_\theta)] \\ \tilde{w}_l(z_\theta) &= -[w_l(z_\theta) + w_l^*(z_\theta)] \end{aligned} \tag{18}$$

Using(14) and (17):

$$\begin{aligned} & m_m r_m^2\ddot{\theta} + D_\theta\dot{\theta} + S\theta + \tfrac{1}{2}\phi_r^T(z_\theta)w_r^*(z_\theta) + \tfrac{1}{2}\phi_l^T(z_\theta)w_l^*(z_\theta) + \lambda_\theta = \\ & -K_p\theta - I_\theta + I_{eq}(0,0) - K_d\dot{\theta} - \tfrac{1}{2}\phi_r^T(z_\theta)w_r(z_\theta) - \tfrac{1}{2}\phi_l^T(z_\theta)w_l(z_\theta) \end{aligned} \tag{19}$$

The lower bound of λ_θ which is nonlinear in nature is illustrated as:

$$\int_0^t \lambda_\theta d\theta = \int_0^t F_{\theta ta} d\theta - \int_0^t f_{\theta e} d\theta - \left[\frac{1}{2}\int_0^t \phi_r^T(z_\theta)w_r(z_\theta)d\theta + \frac{1}{2}\int_0^t \phi_l^T(z_\theta)w_l(z_\theta)d\theta\right. \tag{20}$$

The lower bounds are $\int_0^t F_{\theta ta} d\theta = -\bar{F}_{\theta ta}$ and $\int_0^t f_{\theta e} d\theta = -\bar{f}_{\theta e}$. Also, the Gaussian functions are represented by $\phi_r^T(z_\theta)$ and $\phi_l^T(z_\theta)$, so:

$$\frac{1}{2}\left[\int_0^t \phi_r^T(z_\theta)w_r(z_\theta)d\theta + \int_0^t \phi_l^T(z_\theta)w_l(z_\theta)d\theta\right] = \frac{\sqrt{\pi}}{4} erf(z_\theta)\left[w_r(z_\theta) + w_l(z_\theta)\right] \tag{21}$$

Now the modeling error λ_θ is Lipschitz over a, b such that:

$$\|\lambda_\theta(a) - \lambda_\theta(b)\| \leq L_\theta \|a - b\| \tag{22}$$

where L_θ is the Lipschitz constant. So using (20) and (22):

$$L_\theta = -\bar{F}_{\theta ta} - \bar{f}_{\theta e} - \frac{\sqrt{\pi}}{4} erf(z_\theta)\left[w_r(z_\theta) + w_l(z_\theta)\right]$$

Also to prove the stability of the T2-F-PID control, the property of Eigen value should be considered and stated as:

$$0 < \lambda_m(m_m r_m^2) \leq r_m^2 \|m_m\| \leq \lambda_M(m_m r_m^2) \leq r_m^2 \bar{m} \tag{23}$$

where the min and max eigenvalues of the matrix m_m are represented by $\lambda_m(m_m)$ and $\lambda_M(m_m)$ respectively, also $r_m^2 \bar{m} > 0$ is the upper bound.

The following theorem gives the stability analysis of T2-F-PID controller (13).

Theorem 1 *If the T2-F-PID controller (13) is use to control a closed loop manipulator system (4), then the asymptotic stabilty of the system is assured when the fuzzy laws are*

$$\begin{array}{l} \frac{d}{d\theta}\tilde{w}_r(z_\theta) = -\frac{\eta_1 r_m^2}{t_1}\left[(\dot{\theta} + \rho_\theta \theta)^T \phi_r^T(z_\theta)\right]^T \\ \frac{d}{d\theta}\tilde{w}_l(z_\theta) = -\frac{\eta_2 r_m^2}{t_2}\left[(\dot{\theta} + \rho_\theta \theta)^T \phi_l^T(z_\theta)\right]^T \end{array} \tag{24}$$

and the PID control gains are within the range as

$$\begin{array}{l} \lambda_m\left(K_p\right) \geq \frac{2}{\rho_\theta}\lambda_M(K_i) + \lambda_M(D_\theta) + L_\theta + \frac{2}{\rho_\theta}\Gamma_M \\ \lambda_M(K_i) \leq \frac{\sqrt{\lambda_m(K_p)^3}\sqrt{\lambda_m(m_m)}}{10.4(\lambda_M(m_m))} \\ \lambda_m\left(K_d\right) \geq \frac{\rho_\theta}{2}\lambda_M(m_m) - \Gamma_M - \frac{\rho_\theta}{2}\lambda_M(D_\theta) - \lambda_m(D_\theta) \end{array} \tag{25}$$

where λ_m *and* λ_M *are the minimum and maximum eigenvalues of the matrices.*

Proof Here the Lyapunov candidate is defined as

$$\begin{array}{c} V_\theta = \frac{1}{4}\dot{\theta}^T m_m \dot{\theta} + \frac{1}{4}\theta^T K_p \theta + \frac{\rho_\theta}{4} I_\theta^{*T} K_i^{-1} I_\theta^* + \theta^T I_\theta^* + \frac{\rho_\theta}{4}\theta^T m_m \dot{\theta} + \frac{\rho_\theta}{4}\theta^T K_d \theta \\ + \frac{1}{2r_m^2}\int_0^t \lambda_\theta d\theta - L_\theta + \frac{t_1}{8\eta_1}[\tilde{w}_r^T(z_\theta)\tilde{w}_r(z_\theta)] + \frac{t_2}{8\eta_2}[\tilde{w}_l^T(z_\theta)\tilde{w}_l(z_\theta)] \end{array} \tag{26}$$

It is obvious that $V_\theta(0) = 0$. For validating $V_\theta \geq 0$, V_θ is distributed in three separate parts in such a manner that $V_\theta = V_{\theta 1} + V_{\theta 2} + V_{\theta 3}$

$$\begin{array}{l} V_{\theta 1} = \frac{1}{12}\theta^T K_p \theta + \frac{\rho_\theta}{4}\theta^T K_d \theta + \int_0^t \lambda_\theta d\theta - L_\theta \\ \frac{t_1}{8\eta_1}[\tilde{w}_r^T(z_\theta \tilde{w}_r(z_\theta)] + \frac{t_2}{8\eta_2}[\tilde{w}_l^T(z_\theta)\tilde{w}_l(z_\theta)] \geq 0, \end{array} \tag{27}$$

The above condition is true because $K_p > 0, K_d > 0$ and $\| \tilde{w}_r(z_\theta) \|^2 > 0, \| \tilde{w}_l(z_\theta) \|^2 > 0$.

$$\begin{array}{l} V_{\theta 2} = \frac{1}{12}\theta^T K_p \theta + \frac{\rho_\theta}{4} I_\theta^{*T} K_i^{-1} I_\theta^* + \theta^T I_\theta^* \\ \geq \frac{1}{4}\left[\frac{1}{3}\lambda_m(K_p)\|\theta\|^2 + + \rho_\theta \lambda_m(K_i^{-1})\|I_\theta^*\|^2 - 4\|\theta\|\|I_\theta^*\|\right] \end{array} \tag{28}$$

When $\rho_\theta \geq \frac{12}{\lambda_m(K_p)\lambda_m(K_i^{-1})}$

$$V_{\theta 2} \geq \frac{1}{4}\left(\sqrt{\frac{\lambda_m(K_p)}{3}}\,\|\theta\| - 2\sqrt{\frac{3}{\lambda_m(K_p)}}\,\|I_\theta^*\|\right)^2 \geq 0 \tag{29}$$

and

$$V_{\theta 3} = \frac{1}{12}\theta^T K_p \theta + \frac{1}{4}\dot{\theta}^T m_m \dot{\theta} + \frac{\rho_\theta}{4}\theta^T m_m \dot{\theta} \tag{30}$$

Utilizing the inequality equations

$$\Delta^T \Gamma \Omega \geq \|\Delta\|\,\|\Gamma\Omega\| \geq \|\Delta\|\,\|\Gamma\|\,\|\Omega\| \geq \lambda_M(\Gamma)\,\|\Delta\|\,\|\Omega\| \tag{31}$$

in (30):

$$V_{\theta 3} \geq \frac{1}{4}\left(\frac{1}{3}\lambda_m(K_p)\,\|\theta\|^2 + \lambda_m(m_m)\left\|\dot{\theta}\right\|^2 + \rho_\theta \lambda_M(m_m)\,\|\theta\|\left\|\dot{\theta}\right\|\right) \tag{32}$$

when

$$\rho_\theta \leq \frac{2}{\sqrt{3}}\frac{\sqrt{\lambda_m(m_m)\lambda_m(K_p)}}{\lambda_M(m_m)}$$

$$V_{\theta 3} \geq \frac{1}{4}\left(\sqrt{\frac{\lambda_m(K_p)}{3}}\,\|\theta\| + \sqrt{\lambda_m(m_m)}\left\|\dot{\theta}\right\|\right)^2 \geq 0 \tag{33}$$

Using (27), (29), and (33): $V_\theta = V_{\theta 1} + V_{\theta 2} + V_{\theta 3} \geq 0$. Now we have,

$$\frac{2}{\sqrt{3}}\frac{\sqrt{\lambda_m(m_m)\lambda_m(K_p)}}{\lambda_M(m_m)} \geq \mu_x \geq \frac{12}{\lambda_m(K_p)\lambda_m(K_i^{-1})} \tag{34}$$

Using the relation $\lambda_m(K_i^{-1}) = \frac{1}{\lambda_M(K_i)}$ in (34):

$$\begin{gathered}\frac{\sqrt{\lambda_m(m_m)}}{\lambda_M(m_m)} \geq \frac{6\sqrt{3}\lambda_M(K_i)}{\sqrt{\lambda_m(K_p)}\lambda_m(K_p)} \\ \lambda_M(K_i) \leq \frac{\sqrt{\lambda_m(K_p)^3}\sqrt{\lambda_m(m_m)}}{10.4(\lambda_M(m_m))}\end{gathered} \tag{35}$$

The derivative of (26) is

$$\begin{aligned}\dot{V}_\theta = &\tfrac{1}{2r_m^2}\dot{\theta}^T[-D_\theta\dot{\theta} - S\theta - \tfrac{1}{2}\phi_r^T(z_\theta)w_r^*(z_\theta) - \tfrac{1}{2}\phi_l^T(z_\theta)w_l^*(z_\theta) - \lambda_\theta \\ &-K_p\theta - I_\theta + I_{eq}(0,0) - K_d\dot{\theta} - \tfrac{1}{2}\phi_r^T(z_\theta)w_r(z_\theta) - \tfrac{1}{2}\phi_l^T(z_\theta)w_l(z_\theta)] \\ &+\tfrac{1}{2}\dot{\theta}^T K_p\theta + \tfrac{\rho_\theta}{2}\tfrac{d}{d\theta}{I_\theta^*}^T K_i^{-1} I_\theta^* + \theta^T\tfrac{d}{d\theta}I_\theta^* + \dot{\theta}^T I_\theta^* + \tfrac{1}{2r_m^2}\dot{\theta}^T\lambda_\theta \\ &+\tfrac{\rho_\theta}{2r_m^2}\theta^T[-D_\theta\dot{\theta} - S\theta - \tfrac{1}{2}\phi_r^T(z_\theta)w_r^*(z_\theta) - \tfrac{1}{2}\phi_l^T(z_\theta)w_l^*(z_\theta) - \lambda_\theta \\ &-K_p\theta - I_\theta + I_{eq}(0,0) - K_d\dot{\theta} - \tfrac{1}{2}\phi_r^T(z_\theta)w_r(z_\theta) - \tfrac{1}{2}\phi_l^T(z_\theta)w_l(z_\theta)] \\ &+\tfrac{\rho_\theta}{2}\dot{\theta}^T m_m\dot{\theta} + \tfrac{\rho_\theta}{2}\dot{\theta}^T K_d\theta + \tfrac{t_1}{4\eta_1}[\tfrac{d}{d\theta}\tilde{w}_r^T(z_\theta)\tilde{w}_r(z_\theta)] + \tfrac{t_2}{4\eta_2}[\tfrac{d}{d\theta}\tilde{w}_l^T(z_\theta)\tilde{w}_l(z_\theta)]\end{aligned} \tag{36}$$

Let us consider $\tilde{w}_r(z_\theta) = -\left[w_r(z_\theta) + w_r^*(z_\theta)\right], \tilde{w}_l(z_\theta) = -\left[w_l(z_\theta) + w_l^*(z_\theta)\right]$. Also considering the fuzzy methodology, if the updated law are selected in the manner mentioned below:

$$\begin{array}{c} \frac{d}{d\theta}\tilde{w}_r(z_\theta) = -\frac{\eta_1 r_m^2}{t_1}\left[(\dot{\theta} + \rho_\theta\theta)^T\phi_r^T(z_\theta)\right]^T \\ \frac{d}{d\theta}\tilde{w}_l(z_\theta) = -\frac{\eta_2 r_m^2}{t_2}\left[(\dot{\theta} + \rho_\theta\theta)^T\phi_l^T(z_\theta)\right]^T \end{array} \quad (37)$$

then (36) becomes

$$\begin{array}{c} \dot{V}_\theta = \frac{1}{2r_m^2}\dot{\theta}^T[-D_\theta\dot{\theta} - S\theta - -K_p\theta - K_d\dot{\theta} - I_\theta + I_{eq}(0,0)] + \frac{1}{2}\dot{\theta}^T K_p\theta + \frac{\rho_\theta}{2}\frac{d}{d\theta}I_\theta^{*T}K_i^{-1}I_\theta^* \\ +\theta^T\frac{d}{d\theta}I_\theta^* + +\dot{\theta}^T I_\theta^* + +\frac{\rho_\theta}{2}\dot{\theta}^T m_m\dot{\theta} + \frac{\rho_\theta}{2}\dot{\theta}^T K_d\theta \\ +\frac{\rho_\theta}{2r_m^2}\theta^T[-D_\theta\dot{\theta} - S\theta - \lambda_\theta - K_p\theta - K_d\dot{\theta} - I_\theta + I_{eq}(0,0)] \end{array}$$

As $I_\theta^* = I_\theta - \lambda_\theta(0,0)$and $\frac{d}{d\theta}I_\theta^* = K_i\theta$ therefore, $\frac{d}{d\theta}I_\theta^{*T}K_i^{-1}I_\theta^* = \theta^T I_\theta^*$,$\theta^T\frac{d}{d\theta}I_\theta^* = \theta^T K_i\theta$. Also, $r_m \approx 1$

$$\begin{array}{c} \dot{V}_\theta = -\frac{1}{2}\dot{\theta}^T[D_\theta\dot{\theta} + S\theta + K_d\dot{\theta} - \frac{\rho_\theta}{2}m_m\dot{\theta}]- \\ -\frac{\rho_\theta}{2}\theta^T[D_\theta\dot{\theta} + S\theta + K_p\theta] + \theta^T K_i\theta + \frac{\rho_\theta}{2}\theta^T[I_{eq}(0,0) - I_\theta] \end{array} \quad (38)$$

Using the Lipschitz condition (22) and the property $N^T D + D^T N \leq N^T\Phi N + D^T\Phi^{-1}D$,

$$\begin{array}{c} \frac{\rho_\theta}{2}\theta^T[I_{eq}(0,0) - I_\theta] \leq \frac{\rho_\theta}{2}L_\theta\left\|\theta\right\|^2 \\ -\frac{\rho_\theta}{2}\theta^T D_\theta\dot{\theta} \leq \frac{\rho_\theta}{2}\lambda_M(D_\theta)(\theta^T\theta + \dot{\theta}^T\dot{\theta}) \\ -\frac{\rho_\theta}{2}\dot{\theta}^T S\theta \leq \Gamma_M(\theta^T\theta + \dot{\theta}^T\dot{\theta}), \Gamma_M \leq \lambda_M(S) \end{array} \quad (39)$$

Using (39) and (23) in (38):

$$\begin{array}{c} \dot{V}_\theta \leq -\dot{\theta}^T\left[\lambda_m(D_\theta) + \lambda_m(K_d) - \frac{\rho_\theta}{2}\lambda_M(m_m) - \Gamma_M - \frac{\rho_\theta}{2}\lambda_M(D_\theta)\right]\dot{\theta} \\ -\theta^T\left[\frac{\rho_\theta}{2}\lambda_m(K_p) + \frac{\rho_\theta}{2}\lambda_m(S) - \lambda_M(K_i) - \frac{\rho_\theta}{2}\lambda_M(D_\theta) - \frac{\rho_\theta}{2}L_\theta - \Gamma_M\right]\theta \end{array} \quad (40)$$

The stabilty conditions are justified (40), if

1)

$$\lambda_m(D_\theta) + \lambda_m(K_d) \geq \frac{\rho_\theta}{2}\lambda_M(m_m) - \Gamma_M - \frac{\rho_\theta}{2}\lambda_M(D_\theta) \quad (41)$$

2)

$$\frac{\rho_\theta}{2}[\lambda_m(K_p) + \lambda_m(S)] \geq \lambda_M(K_i) + \frac{\rho_\theta}{2}\lambda_M(D_\theta) + \frac{\rho_\theta}{2}L_\theta + \Gamma_M \quad (42)$$

From the stabilty conditions and (35), the ranges of gains are:

$$\begin{array}{c} \lambda_m(K_p) \geq \frac{2}{\rho_\theta}\lambda_M(K_i) + \lambda_M(D_\theta) + L_\theta + \frac{2}{\rho_\theta}\Gamma_M \\ \lambda_m(K_d) \geq \frac{\rho_\theta}{2}\lambda_M(m_m) - \Gamma_M - \frac{\rho_\theta}{2}\lambda_M(D_\theta) - \lambda_m(D_\theta) \\ \lambda_M(K_i) \leq \frac{\sqrt{\lambda_m(K_p)^3}\sqrt{\lambda_m(m_m)}}{10.4(\lambda_M(m_m))} \end{array} \quad (43)$$

So the controller will generate stable control forces when the gains are selected from the stability zones as represented by (43)

4 Analysis and Validation

Manipulator parameters are obtained from [23, 45] in order to confirm the capability and performance of the proposed fuzzy PID controller. These parameters are used to simulate the manipulator process and to achieve the motion with vibration control. Such parameters are used to model the process of the manipulator. They are also used to obtain the motion with a controlled vibration. The various parameters linked to the system are illustrated in the Table1.

Table 1	Simulation Parameters
Mass (m_m, kg)	2
Spring Constant $(S, N/m)$	5×10^3
Damping Constant $(D_\theta, Ns/m)$	9
TA Fricton Coefficient (Nm/rad)	0.95
TA Motor Torque Constant (Nm/V)	0.06
TA Encoder Gain (V/rad)	0.3979

The input nonlinearity for the purpose of the simulation is the Coulomb friction[46] associated with the manipulator's torsional motion .The friction of the Coulomb is of a nonlinear type:

$$FC_{sim} = \alpha_0 sgn(\dot{\theta}) + \alpha_1 (\exp)^{-\alpha_2 |\dot{\theta}|} sgn(\dot{\theta}) \quad (44)$$

where $\alpha_0, \alpha_{1,} \alpha_2$ are the friction constants and $\dot{\theta}$ is the velocity of the manipulator. The simulation of the manipulator is done using the Matlab/Simulink platform. Simulink program is used to create different simulations to show the adequate vibration attenuation of the agricultural manipulator can be accomplished by using the T2-F-PID controller. The vibration attenuation capabilities of the indicated controller are contrasted with the basic PD/PID and T1-F-PID controllers to check the efficiency of the T2-F-PID controller. A PD controller is of the form:

$$\mathbf{u}_{pd} = -K_p \mathbf{e} - K_d \dot{\mathbf{e}} \quad (45)$$

K_p and K_d are the gains as stated earlier.The error e is illustrated as $e = \theta - \theta^d, \dot{e} = \dot{\theta} - \dot{\theta}^d$. For the reference, $\theta^d = \dot{\theta}^d = 0$. The simulations for generating vibration control plots are carried out for the period of 6 s. For the simulation purpose, the weight of the *TA* is taken 5% of the manipulator weight. For comparing the results depicting vibration attenuation, dual subsystem simulink blocks for manipulator dynamics are created. One block is developed without control system ans the other with the control system. The inputs for the manipulator dynamics are sinusoidal signal and the Coulomb friction which is nonlinear in nature as stated in (44). The frequency value associated with the simulation is set to 300 rad/s.The acceleration signals generated from the manipulator dynamics blocks are fed to the series of numerical integrators to extract velocity signals and position signals respectively. Overall four tests are performed in Simulink: 1. PD Control, 2. PID Control, 3. T1-F-PID Control and 4. T2-F-PID Control. For T1-F-PID Control, the integrated type-1 fuzzy toolbox for Matlab/Simulink is utilized, whereas for T2-F-PID Control the open source Type-2 fuzzy toolbox [47] is utilized for accomplishing fuzzy techniques. The generated control signals from the controller block is transmitted to the TA for the vibration control in the manipulator. The inputs: position error and velocity error, are considered to be Gaussian membership functions. Four membership functions are allocated for position error whereas three membership functions are allocated for velocity error. Normalization are set as $[-\mathbf{1},\mathbf{1}]$.The type-2 fuzzy system is defuzzified using Karnik-Mendel technique [32]. For type-2 fuzzy system, six IF-THEN rules are sufficient to maintain the regulation error. Ten IF-THEN rules suffices the maintaining of minimal regulation error in case of type-1 fuzzy system. The technique of Gaussian functions is introduced for type-1 fuzzy logic. Both type-1/type-2 fuzzy system are based on IF-THEN rules illustrated by:

$$\begin{array}{lll} IF & \theta & is \;\; \Psi_1 \\ AND\ \dot{\theta} & & is \;\; \Psi_2 \\ THEN\ u_\theta & & is \;\; \Psi_3 \end{array} \tag{46}$$

where θ is the position error, $\dot{\theta}$ is the velocity error, and u_θ is the required control force. Ψ_1, Ψ_2,and $\Psi_3$are the fuzzy sets. The design parameters are, $\frac{\eta_1}{t_1} = \frac{\eta_2}{t_2} = 8$. From Theorem 1., it is evident that the ranges of the gains can be identified. So, based on the ranges of PID gains and substituting the parameters from Table 1 to the equation 25, the following ranges of gains are extracted:

$$\lambda_m(K_p) \geq 219, \lambda_m\left(K_d\right) \geq 69, \lambda_M(K_i) \leq 2500 \tag{47}$$

After attempting several trials with the gains based on eqn. (47), it is observed that for PD, PID, T1-F-PID and T2-F-PID controller the most suited gains for efficient vibration attenuation as well as stability are:

$$\lambda_{\min}(K_p) = 273, \lambda_m\left(K_d\right) = 81, \lambda_M(K_i) = 1690 \tag{48}$$

Also, some tested were carried out by selecting the values from the ranges different from the ones extracted by the Theorem 1. For validation we selected the gains from the ranges: Proportional gain less than 219, Derivative gain less than 69 and proportional gain greater than 2500. It is observed that for each and every test with the increasing gains from that zone, the results were unstable adding more vibration to the manipulator. So, all the result was discarded from the unstable zones.

To validate the performance of the controllers, the vibration attenuation comparisons is carried out among PD, PID, T1-F-PID and T2-F-PID controllers which are displayed in Fig. 9 - Fig. 12. The outcomes of the average vibration attenuation is computed by implementing mean squared error illustrated as $MSE = \frac{1}{dat}\sum_{k=1}^{d} \theta\left(k\right)^2$,where the chatter vibration is depicted by $\theta\left(k\right)$. The total data is illustrated by dat. The data of the average vibration attenuation is shown in Table 2.

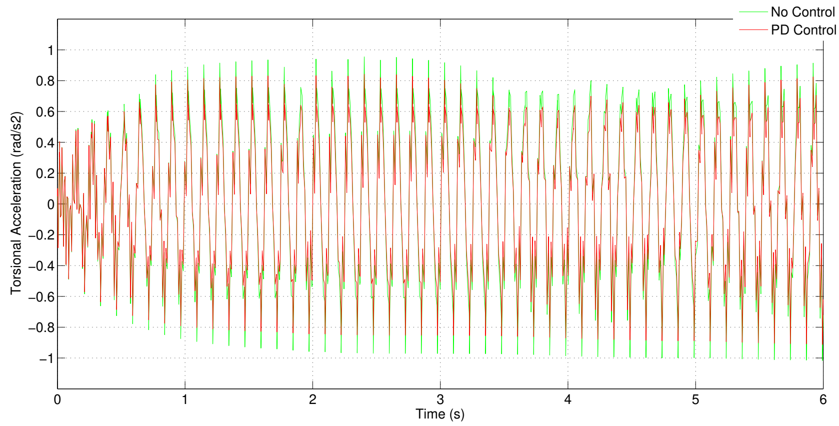

Fig. 9 Manipulator vibration control using PD controller

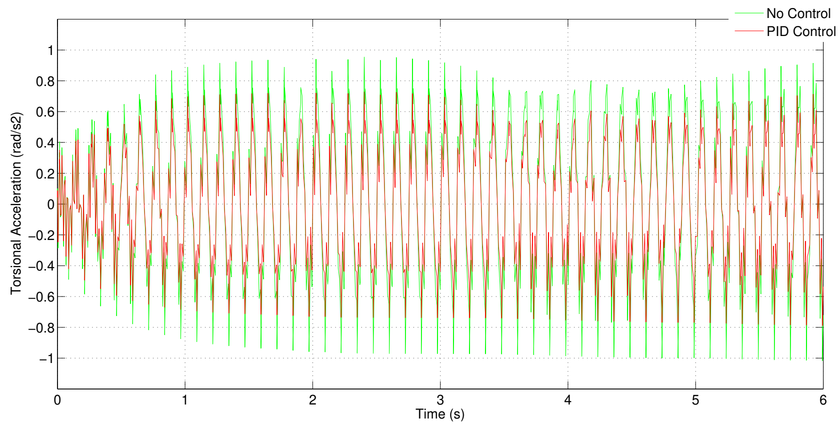

Fig. 10 Manipulator vibration control using PID controller

$Table2 : Averagevibrationattenuation, MSEindicator$

No ctrl.	*PD*	*PID*	T1-F-PID	T2-F-PID
0.6505	0.5010	0.4113	0.1763	0.0998

From, Table 2 it is validated that T2-F-PID is the superior among all the controllers in vibration attenuation.The Fig. 13 depicts the control signal plot of T2-F-PID controller. In Fig. 14, the plot of TA control force is illustrated.

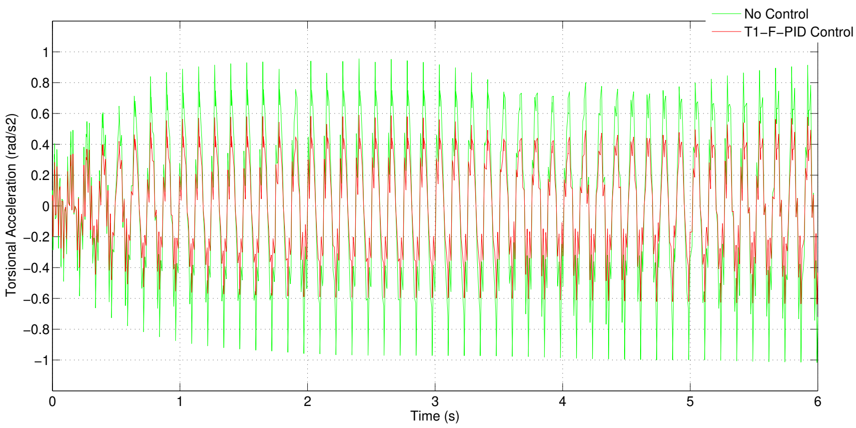

Fig. 11 Manipulator vibration control using T1-F-PID controller

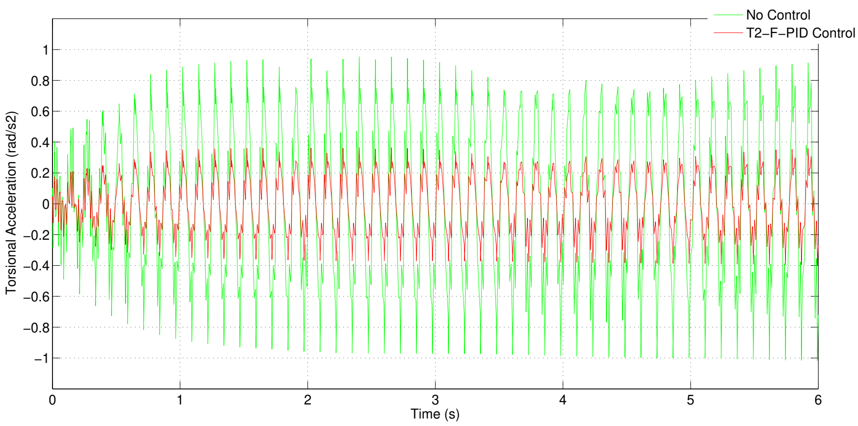

Fig. 12 Manipulator vibration control using T2-F-PID controller

5 Conclusion

In this work, the stabilization and the control of the vibration related to the mechanical manipulator arm is verified and validated when the present configuration is meant to be automated as needed for agricultural applications. The camera setup, when mounted with such motorized arm, will incur tremendous vibrations. This sort of vibration experienced hinders the quality of the acquired data. To achieve this we used a conventional PID controller in combination with the type-2 fuzzy logic (T2-F-PID). The PID controller produces the key control operation, while the nonlinear compensation is dealt with by means of the fuzzy logic of type-2. For active vibration control, the torsion actuator (TA) movement is simulated. The result obtained by the simulation

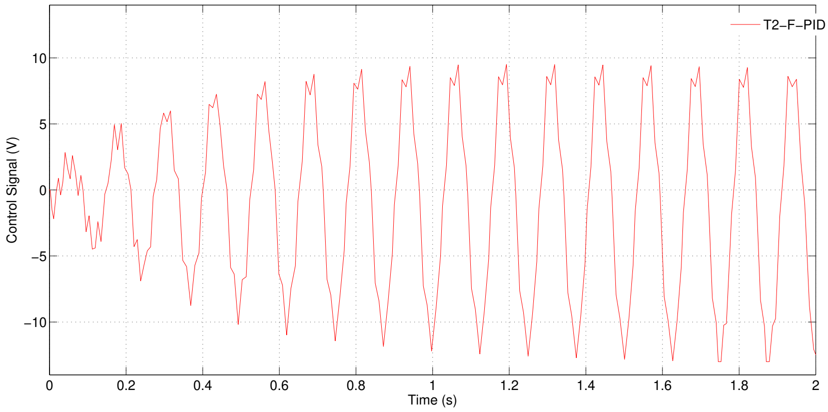

Fig. 13 T2-F-PID control signal

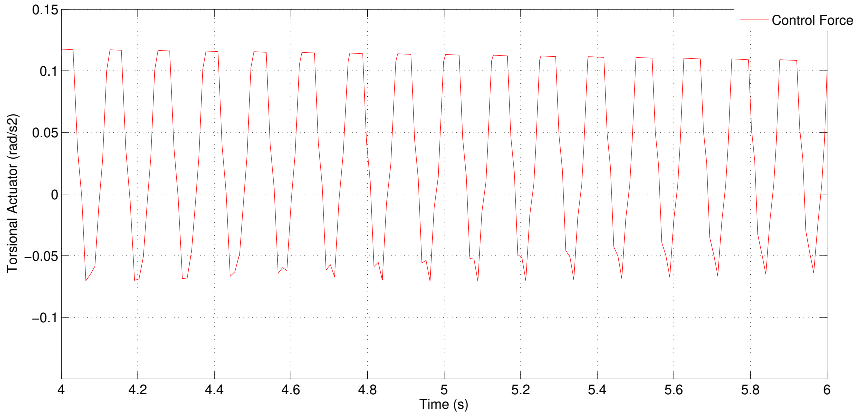

Fig. 14 Torsional actuator control force

of T2-F-PID is compared with both simple PD/PID controller and T1-F-PID controller. The consequence of the study validates that T2 F-PID is the best of all the controllers to achieve proper vibration attenuation. The future work is intended towards the effective design of TA for better efficiency. Also, we aim to compare the effectiveness of T2-F-PID with Sliding Mode Controller (SMC).

Acknowledgment

The authors are thankful to Örebro University for reference of the logistics as a part of this study.

Author Contributions

Idea, S.P., A.A., D.K.; Investigation, S.P., A.A.,D.K.; Model Validation, S.P., A.A.,D.K.; Writing-draft, review and editing, S.P., A.A.,D.K.

Conflict of Interests

The authors declare no conflict of interests.

References

1. Ehrhardt, D. W., and Frommer, W. B. "New technologies for 21st century plant science". The Plant cell, 24(2), 374–394, 2012.
2. "GROWBOX" [Online]. Available: https://en.wikipedia.org/wiki/Grow_box.
3. "FARM BOT" [Online]. Available: https://farm.bot/.
4. M. Barrasso, "Autonomous Plant Growing System," 2016.
5. "LOMAS++ – Sweden's Testbed in AI and Autonomous Systems" [Online]. Available: http://platformaimee.se/?p=1031
6. "Orebro Universitet" [Online]. Available: https://www.oru.se/
7. Li. L, Zhang. Q and Huang.D, "A Review of Imaging Techniques for Plant Phenotyping", Sensors 14, 20078 - 20111, 2014.
8. Sakurai. S, Uchiyama. H, Shimada. A, Arita. D and Rin-ichiro Taniguchi. R, "Two-step Transfer Learning for Semantic Plant Segmentation", ICPRAM, 2018.
9. Sakurai, S., Uchiyama, H., Shimada, A., Taniguchi, R. I, "Plant growth prediction using convolutional LSTM", VISIGRAPP, 5, 105-113, 2019.
10. Shamshiri R R, Weltzien C, Hameed I A, Yule I J, Grift T E, Balasundram S K, et al., "Research and development in agricultural robotics: A perspective of digital farming", Int J Agric Biol Eng, 11(4), 1–14, 2018.
11. Roshanianfard A, Noguchi N, Kamata T., "Design and performance of a robotic arm for farm use", Int J Agric Biol Eng, 12(1), 146–158, 2019.
12. "ROBOTICS - INTRODUCTION" Available: http://www.site.uottawa.ca/ petriu/CEG4392-IntroRobotics-Arms.pdf
13. Oh. T, Park. J, Seshadrinathan. K, Lee. S and Bovik. A. C., "No-Reference Sharpness Assessment of Camera-Shaken Images by Analysis of Spectral Structure," in IEEE Transactions on Image Processing, vol. 23, no. 12, pp. 5428-5439, Dec. 2014.
14. Nguyen M.T., Yuan C., Huang J.H., "Kinematic Analysis of A 6-DOF Robotic Arm". Advances in Mechanism and Machine Science, vol 73, 2019.
15. Leugering. G, "Control and stabilization of a flexible robot arm", Dynamics and Stability of Systems, 5:1, 37-46, 1990.
16. Singh. S. N, "Control and stabilization of nonlinear uncertain elastic robotic arm," IEEE Transactions on Aerospace and Electronic Systems, vol. 24, no. 2, pp. 148-155, March 1988.
17. Etxebarria. V, Arantza. S, and Ibone. L, "Control of a Lightweight Flexible Robotic Arm Using Sliding Modes", International Journal of Advanced Robotic Systems, Volume 2, Number 2, pp. 103 - 110, 2005.
18. Khalil. FF and Khalil EF, "Journal of Engineering and Development", Vol. 17, No.3, 183-198, August 2013.
19. W. He, Y. Ouyang and J. Hong, "Vibration Control of a Flexible Robotic Manipulator in the Presence of Input Deadzone," in IEEE Transactions on Industrial Informatics, vol. 13, no. 1, pp. 48-59, Feb. 2017.
20. Z-C. Qiu, Adaptive nonlinear vibration control of a Cartesian flexible manipulator driven by a ballscrew mechanism, Mechanical Systems and Signal Processing, Volume 30, 2012, Pages 248-266.

21. Wei, J., Qiu, Z., Han, J. et al. Experimental Comparison Research on Active Vibration Control for Flexible Piezoelectric Manipulator Using Fuzzy Controller. J Intell Robot Syst 59, 31–56 (2010).
22. Liu Z., Liu J. (2020) Dynamic Modeling and Vibration Control for a Nonlinear Three-Dimensional Flexible Manipulator. In: PDE Modeling and Boundary Control for Flexible Mechanical System. Springer Tracts in Mechanical Engineering. Springer, Singapore.
23. Yavuz, Scedil., Malgaca, L., Karagülle, H., Vibration control of a single-link flexible composite manipulator, Composite Structures (2016).
24. Matsumori, H., Deng, M-C., and Noge, Y, An Operator-based Nonlinear Vibration Control System Using a Flexible Arm with Shape Memory Alloy. International Journal of Automation and Computing, 17(1), 2020.
25. W. Deng, H. Liu, J. Xu, H. Zhao and Y. Song, "An Improved Quantum-Inspired Differential Evolution Algorithm for Deep Belief Network," in IEEE Transactions on Instrumentation and Measurement, 2020.
26. S. Tong, X. Min and Y. Li, "Observer-Based Adaptive Fuzzy Tracking Control for Strict-Feedback Nonlinear Systems With Unknown Control Gain Functions," in IEEE Transactions on Cybernetics, vol. 50, no. 9, pp. 3903-3913, Sept. 2020
27. Tong, S., Li, Y. Robust adaptive fuzzy backstepping output feedback tracking control for nonlinear system with dynamic uncertainties. Sci. China Inf. Sci. 53, 307–324 (2010).
28. Fu-Cai Liu, Li-Huan Liang and Juan-Juan Gao. Fuzzy PID Control of Space Manipulator for Both Ground Alignment and Space Applications. International Journal of Automation and Computing, vol. 11, no. 4, pp. 353-360, 2014.
29. Khaled M. Goher and Sulaiman O. Fadlallah. Control of a Two-wheeled Machine with Two-directions Handling Mechanism Using PID and PD-FLC Algorithms. International Journal of Automation and Computing, vol. 16, no. 4, pp. 511-533, 2019.
30. R.I John, P.R Innocent, M.R Barnes,Neuro-fuzzy clustering of radiographic tibia image data using type 2 fuzzy sets, Information Sciences, Volume 125, Issues 1–4, 2000, Pages 65-82.
31. Mendel, J.M.Uncertain Rule-Based Fuzzy Logic Systems: Introduction and New Directions; Prentice Hall PTR:Upper Saddle River, NJ, USA, 2001.
32. Liang, Q.; Mendel, J.M. Interval type-2 Fuzzy Logic Systems: Theory and Design.IEEE Trans. Fuzzy Syst.2002,8, 535–550.
33. Sepúlveda, R.; Castillo, O.; Melin, P.; Rodríguez-Díaz, A.; Montiel, O. Experimental Study of Intelligent Controllers Under Uncertainty using type-1 and type-2 Fuzzy Logic,Inf. Sci.2007,177, 2023–2048.
34. Paul, S.; Yu, W.; Li, X.; Bidirectional active control of structures with type-2 fuzzy PD and PID.Int. J. Syst. Sci.2018,49, 766–782.
35. Naik, K. A.; Gupta, C. P. , Performance comparison of type-1 and type-2 fuzzy logic systems. In Proceedingsof the 4th International Conference on Signal Processing,Computing and Control (ISPCC), Solan, India,21–23 September 2017; pp. 72–76.
36. Bai, Y.; Wang, D. On the Comparison of type-1 and Interval type 2 Fuzzy Logic Controllers Used in a LaserTracking System.IFAC-PapersOnLine2018,51, 1548–1553.
37. Sun. D, Liao. Q, Gu. X, Li.C and Ren. H, "Multilateral Teleoperation With New Cooperative Structure Based on Reconfigurable Robots and Type-2 Fuzzy Logic" IEEE Transactions on Cybernetics, Volume: 49, Issue: 8, 2845 - 2859, Aug. 2019.
38. "Franka Emika Robot" [Online].Available: https://www.franka.de/
39. Varde. S, Panse. M.S, "Offline Stereo Camera Calibration of Raspberry Pi Compute Module," International Journal of Latest Technology in Engineering, Management Applied Science, Volume VI, Issue IX, September 2017.
40. Roldan C, Campa FJ, Altuzarra O, et al. (2014) Automatic identification of the inertia and friction of an electromechanical actuator. Mechanisms and Machine Science 17: 409–416
41. Liang, Q., and Mendel, J.M., Interval Type-2 Fuzzy Logic Systems: Theory and Design, IEEE Trans. on Fuzzy Systems, Vol. 8, Issue No.5, pp. *535-550, 2002.*
42. Sepúlveda, R., Castillo, O., Melin, P., Rodríguez-Díaz, A., and Montiel, O., Experimental Study of Intelligent Controllers Under Uncertainty using Type-1 and Type-2 Fuzzy Logic, Information Sciences, Vol. 177, Issue No. 10, pp. 2023–2048, 2007.

43. Castillo, O., Aguilar, L., Cázarez, N., and Melin, P., Systematic Design of a Stable Type-2 Fuzzy Logic Controller, Forging New Frontiers: Fuzzy Pioneers II, Springer Berlin Heidelberg, Vol. 218, pp. 319-331, 2008.
44. Lin, TC., Liu, HL., and Kuo, MJ., Direct Adaptive Interval Type-2 Fuzzy Control of Multivariable Nonlinear Systems, Eng. Applications of Artificial Intelligence, Vol.22, Issue No. 3, pp. 420-430, 2009.
45. M. Hassan, R. Dubay, C. Li, R. Wang, Active vibration control of a flexible one-link manipulator using a multivariable predictive controller, Mechatronics, Volume 17, Issue 6, 2007,Pages 311-323.
46. Jun Oh Jang, Gi Joon Jeon, A parallel neuro-controller for DC motors containing nonlinear friction, Neurocomputing, Volume 30, Issues 1–4, 2000, Pages 233-248.
47. Taskin, A., and Kumbasar, T., An Open Source Matlab/Simulink Toolbox for Interval Type-2 Fuzzy Logic Systems, Proc. of the IEEE symposium series on computational intelligence, pp. 1561–1566, Cape Town, South Africa: IEEE Computational Intelligence Society, IEEE, 2015.